

Peripheral benzodiazepine receptor (PBR) ligand cytotoxicity unrelated to PBR expression

Gregory Hans^{a,b,*}, Sabine Wislet-Gendebien^a, François Lallemand^a,
Pierre Robe^{a,d}, Bernard Rogister^{a,b}, Shibeshih Belachew^{a,b}, Laurent Nguyen^a,
Brigitte Malgrange^a, Gustave Moonen^{a,b}, Jean-Michel Rigo^{a,c}

^aCentre of Cellular and Molecular Neurobiology, Université de Liège, 17 Place Delcour, 4020 Liège 2, Belgium

^bDepartment of Neurology, Université de Liège, 13 Avenue de l'Hôpital, 4000 Liège 1, Belgium

^cDepartment of Physiology, Transnationale universiteit Limburg/Limburgs Universitair Centrum,
biomedisch onderzoeksinstituut, B-3590 Diepenbeek, Belgium

^dDepartment of Neurosurgery, Université de Liège, 13 Avenue de l'Hôpital, 4000 Liège 1, Belgium

Received 13 September 2004; accepted 29 November 2004

Abstract

Some synthetic ligands of the peripheral-type benzodiazepine receptor (PBR), an 18 kDa protein of the outer mitochondrial membrane, are cytotoxic for several tumor cell lines and arise as promising chemotherapeutic candidates. However, conflicting results were reported regarding the actual effect of these drugs on cellular survival ranging from protection to toxicity. Moreover, the concentrations needed to observe such a toxicity were usually high, far above the affinity range for their receptor, hence questioning its specificity. In the present study, we have shown that micromolar concentrations of FGIN-1-27 and Ro 5-4864, two chemically unrelated PBR ligands are toxic for both PBR-expressing SK-N-BE neuroblastoma cells and PBR-deficient Jurkat lymphoma cells. We have thereby demonstrated that the cytotoxicity of these drugs is unrelated to their PBR-binding activity. Moreover, Ro 5-4864-induced cell death differed strikingly between both cell types, being apoptotic in Jurkat cells while necrotic in SK-N-BE cells. Again, this did not seem to be related to PBR expression since Ro 5-4864-induced death of PBR-transfected Jurkat cells remained apoptotic. Taken together, our results show that PBR is unlikely to mediate all the effects of these PBR ligands. They however confirm that some of these ligands are very effective cytotoxic drugs towards various cancer cells, even for reputed chemoresistant tumors such as neuroblastoma, and, surprisingly, also for PBR-lacking tumor cells.

© 2004 Elsevier Inc. All rights reserved.

Keywords: Peripheral benzodiazepine receptor; Apoptosis; Cancer; Ligands; Mitochondrion; Necrosis

1. Introduction

Peripheral benzodiazepine receptor-type is an 18 kDa protein of the outer mitochondrial membrane [1]. Initially described as a binding site for benzodiazepines outside the nervous system [2], it was later demonstrated to be expressed in most mammalian tissues [3]. The exact function of the PBR remains a matter of debate but it is

believed to play a role in several physiological and pathological processes including steroidogenesis, cellular growth and differentiation, immunomodulation, oxygen consumption, and apoptosis [4,5]. Beside its endogenous ligands (diazepam binding inhibitor, porphyrins or cholesterol), several synthetic molecules bind the PBR selectively [6]. These synthetic ligands can be subdivided into three main families: benzodiazepines such as the 4'-chloro derivative of diazepam Ro 5-4864, isoquinoline carboxamides, among which PK11195, and indoacetamide derivatives such as FGIN-1-27 [6]. Many putative roles of this receptor have been inferred from the biological effects of these ligands [7].

In particular, during the last years, many studies have been devoted to the effects of PBR ligands on cell survival,

Abbreviations: $\Delta\Psi_m$, mitochondrial membrane potential; PBR, peripheral benzodiazepine receptor; BA, Bongkrekic acid; CsA, cyclosporin A; MTT, 1-(4,5-dimethylthiazol-2-yl)-3,5-diphenylformazam bromide; mPTP, permeability transition pore; VDAC, voltage-dependent anion channel; PARP, poly(ADP-ribose) polymerase-1; ROS, reactive oxygen species

* Corresponding author. Tel.: +3243665918; fax: +3243665912.

E-mail address: G.hans@teledisnet.be (G. Hans).

and especially to their toxicity towards tumor cell lines [8–12]. The PBR was moreover described to be abundantly expressed in a wide variety of malignant cells, even being the hallmark of cancerogenesis in some tissues, e.g. gliomas [13,14]. In that respect, the level of PBR expression was also suggested to be a clinically relevant prognosis factor [15–17]. Together, these observations led several authors to consider the PBR as a promising drug target, especially in the field of cancer [6,18]. Consistently, many experimental studies suggest that PBR ligands might be good candidates as chemotherapeutic, or at least chemosensitizing, agents [8,9,11,12,19,20].

Nevertheless, the molecular mechanism(s) of PBR ligands-induced cell death remains poorly understood. The most often reported findings suggest apoptosis induction. Indeed, PBR ligands have been demonstrated to induce an activation of caspase-3 [8,10,11,21,22] and caspase-9 [11], a cytosolic release of cytochrome *c* [11,21], an increase in ROS production [23], an activation of p38 MAPK [9] and, finally an opening of the mitochondrial permeability transition pore (mPTP) [8,11,22–24]. This last finding is of particular interest since the PBR is thought to take part in the mPTP [25]. This mPTP is a large molecular complex located at junction sites between the inner and the outer mitochondrial membranes [26,27]. In some circumstances, mPTP opening increases the mitochondrial membrane permeability, allowing the leakage of mitochondrial pro-apoptotic factors such as the cytochrome *c* into the cytosol [28] and disrupting the mitochondrial membrane potential ($\Delta\psi_m$) [29,30]. Such an opening leads either to necrosis if ATP production is severely impaired, or to apoptosis when ATP production remains normal [31]. However, evidences in favour of a direct trigger for a mPTP opening by PBR ligands are weak and the $\Delta\psi_m$ loss reported in those studies is probably a downstream event occurring in many apoptotic processes where mitochondria act as executioners [32,33].

Conversely, other studies aimed at unravelling the action of PBR ligands on cellular survival have not reported toxic but pro-survival effects [34,35].

In this study, we have tried to clarify the role of the PBR in cell death induced by some of its ligands. This issue is indeed essential regarding the potential use of these drugs in therapeutic strategies against cancer. For that purpose, we have compared the toxicity profiles of and the biochemical cascades induced by two chemically unrelated PBR ligands on PBR-expressing and PBR-lacking tumor cell lines, i.e. SK-N-BE neuroblastoma and Jurkat human T leukemia cells, respectively.

2. Methods

2.1. Reagents and antibodies

Ro 5-4864, Bongkreik acid, sodium orthovanadate, sodium fluoride and β -glycerophosphate were all from

Sigma–Aldrich. Anti-PARP, anti-caspase-9 and anti-caspase-3 antibodies were from Santa Cruz biotechnology. Anti-caspase-8 and anti-cytochrome *c* antibodies were from BD Pharmingen. Boc-D-FMK, Z-LETD-FMK, Z-DEVD-CHO, Z-LEDH-FMK, cyclosporine A and anti-VDAC antibody were all from calbiochem. Anti-PBR 8D7 antibody was a kind gift of Dr. P. Casellas (Sanofi-Synthelabo, Montpellier, France).

2.2. Cell culture

Jurkat human T leukemia cells, SK-N-BE human neuroblastoma cells, U-87 and LN-18 human glioma cells were all grown in RPMI 1640 (Invitrogen,) supplemented with fetal calf serum (10%, v/v, Invitrogen), 100 μ g/ml streptomycin, and 100 U/ml penicillin. Cultures were maintained in a humidified atmosphere containing 5% CO₂. Jurkat cells steadily expressing the PBR were a kind gift of Dr. P. Casellas (Sanofi-Synthelabo, Montpellier, France). They were grown in the same medium supplemented with 1 mg/ml G418.

For the induction of cell death, SK-N-BE cells were plated at a density of either 15×10^3 cells per well in 96-wells microplates (Nunc) or 1.5×10^6 cells in 10 cm Petri dishes (Nunc) and allowed to attach for 24 h before treatment. The medium was then replaced by medium containing either the drug(s) at desired concentrations or vehicle(s). Jurkat cells were diluted at a density of 250×10^3 cells/ml in medium supplemented with either drug(s) or vehicle(s).

2.3. Assessment of cell survival

The cell survival was assessed 24 h after the beginning of the exposure to drugs. For SK-N-BE cells, the MTT assay was used [36]. Briefly, the medium was removed and cells were incubated for 2 h at 37 °C with medium supplemented with 0.15 mg/ml 1-(4,5-dimethylthiazol-2-yl)-3,5-diphenylformazam bromide (MTT). Mitochondria of living cells formed a blue precipitate that was dissolved in isopropanol before the absorbance was read using a BiotekEL-309 ELISA reader (test wavelength 540 nm, reference wavelength 650 nm). For Jurkat cells, the LIVE/DEAD[®] assay (Molecular Probes) was used according to the manufacturer's instructions. Briefly, 1 ml of cell suspension was harvested and cells were re-suspended in 500 μ l of PBS containing 1 μ M ethidium homodimer (EthD-1) and 1 μ M calcein AM. EthD-1 is incorporated in dying cells while calcein AM is transformed into the fluorescent calcein by plasma esterases of living cells. Cells were incubated at 37 °C for 30 min before fluorescence was read using a spectra MAX Gemini microplate fluorescence reader (Molecular Devices) with the SoftMax PRO software (excitation at 480 nm and emission at 530 nm for calcein and at 640 nm for EthD-1). Viability was measured as the 530 nm/

640 nm fluorescence ratio and expressed as percentage of the same ratio in controls.

2.4. TUNEL labeling

Internucleosomal cleavage of DNA was assessed by using the terminal deoxynucleotidyltransferase-mediated UTP nick end labeling (TUNEL labeling) assay according to the manufacturer's instructions (Roche). Briefly, cells were fixed with 4% paraformaldehyde for 10 min at room temperature. They were then permeabilized and incubated for 1 h at 37 °C with the terminal deoxynucleotidyltransferase in the presence of fluorescein-labeled nucleotides. The number of labeled cells was manually counted under the control of a fluorescence microscope (Axiovert 135 microscope, 40× objective, Zeiss) for adherent SK-N-BE and measured using the fluorescence microplate reader for Jurkat cell suspensions (excitation at 480 nm and emission at 535 nm).

2.5. DNA ladder

Genomic DNA was extracted from dying SK-N-BE and Jurkat cells and separated on a 2% agarose gel stained with ethidium bromide according to the manufacturer's instructions (Apoptotic DNA ladder kit, Roche). Gels were scanned using a Typhoon 9200 gel scanner (Molecular Dynamics) and analyzed by using the Image Quant[®] software.

2.6. RT-PCR

Analysis of mRNA PBR expression was carried out by RT-PCR. Total RNA was extracted by using the RNeasy extraction minikit (Qiagen). An amount of 1 µg RNA was digested with 1 U of DNase I (Invitrogen) for 15 min at room temperature. Oligo-dT-primers and the SuperScript II reverse transcriptase (Invitrogen) were used for cDNA synthesis. PCR amplification was performed in a volume of 50 µl containing 250 nM of each primer, 20 µM of each dNTP (Amersham), 2.5 mM MgCl₂, and 1.25 U *Taq* Polymerase (Promega, Mannheim). PCR was performed in a Peltier thermal cycler (PTC-200, M. J. Research, USA). Primers used were as follows: (i) for PBR, 5'-TCT-GGA-AAG-AGC-TGG-GAG-G-3' (sense) and 5'-AAG-GCC-AGC-CAG-GCC-AGG-3' (antisense); (ii) for GAPDH, 5'-ACG-ACA-GTC-CAT-GCC-ATC-AC-3' (sense) and 5'-TCC-ACC-ACC-CTG-TTG-CTG-TA-3'. Thermal cycling was as follows: (i) denaturation at 94 °C for 1 min, (ii) annealing at 63 °C for 1 min, (iii) elongation at 72 °C for 40 s, 35 cycles before a final elongation of 7 min at 72 °C. PCR products were then loaded on a 2% agarose electrophoresis gel stained with ethidium bromide (0.5 µg/ml). Gels were scanned with the typhoon gel scanner as described above.

2.7. Western blotting

For PBR detection, cells were harvested and lysed in a buffer containing 63 mM Tris and 1% sodium dodecyl sulfate (SDS), pH 6.8. For all other protein detections, cells were lysed in 25 mM Hepes, 150 mM NaCl, 0.5% Triton, 10% glycerol, 1 mM DTT, 1 mM sodium orthovanadate, 25 mM β-glycerophosphate, 1 mM NaF and complete[®] protease inhibitor cocktail (one tablet for 50 ml; Roche, Brussels, Belgium). The protein content of each lysate was determined by using the Bradford method as previously described [37]. Protein lysates were then mixed with an equal volume of gel loading buffer (20% glycerol, 4% SDS, 100 mM Tris, 5% β-mercaptoethanol and bromophenol blue) before being boiled for 3 min. After boiling, 20 µg of protein were subjected to SDS-PAGE gel electrophoresis (14% polyacrylamide for caspase western blots, 12% for cytochrome *c* and PBR and 10% for PARP). Proteins were then transferred on a PVDF membrane (Amersham) by semi-dry electroblotting in transfer buffer (192 mM glycine, 25 mM Tris and 20% methanol). Blots were then blocked overnight at 4 °C in 10% non-fat dry milk diluted in TBS supplemented with 0.05% Tween-20 (Bio-Rad) (TTBS). The following primary antibodies were incubated for 2 h at room temperature in TTBS supplemented with 5% non-fat dry milk as follows: (a) mouse monoclonal anti-PBR antibody (clone 8D7, kind gift of Dr P. Casellas, Sanofi-Synthelabo, Montpellier, 1:5000), (b) mouse monoclonal anti-cytochrome *c* antibody (clone 7H8.2C12, BD Pharmingen, 1:1000), (c) rabbit polyclonal anti-caspase 3 antibody (sc-7148, Santa Cruz Biotechnology, 1:1000), (d) mouse monoclonal anti-caspase 9 antibody (sc-17784, Santa Cruz Biotechnology, 1:1000), (e) rabbit polyclonal anti-caspase 8 antibody (Catalog N° 559932, BD Pharmingen, 1:1000), (f) polyclonal rabbit anti-PARP antibody (sc-7150, Santa Cruz, 1:1000), (g) mouse monoclonal anti-Porin 31HL antibody (anti-VDAC, Calbiochem, 1:1000), (h) mouse monoclonal anti-β-actin antibody (Sigma-Aldrich, 1:5000). Peroxidase-conjugated secondary antibodies were incubated for 1 h at room temperature as follows: (a) monoclonal anti-rabbit antibody (clone RG-16, Sigma-Aldrich, 1:5000) and (b) goat anti-mouse IgG (Product No. A2304, Sigma-Aldrich, 1:5000). Blots were then washed extensively and developed using enhanced chemoluminescence (Pierce).

2.8. Cell fractionation

Mitochondrial protein isolation was performed as previously described [38]. A 30 × 10⁶ cells were suspended in a sucrose buffer (250 mM sucrose, 1 mM DTT, 10 mM KCl, 1 mM EDTA, 1 mM EGTA, 1.5 mM MgCl₂, 20 mM Hepes, Protease inhibitor cocktail Complete[®] (Roche, Brussels, Belgium)), pH 7.4 at 4 °C and homogenized with

50 strokes in a glass homogenizer. The suspension was then centrifuged at $800 \times g$ for 10 min at 4°C to pellet debris and nuclei. The supernatant was centrifuged again at $150,000 \times g$ for 10 min at 4°C . The mitochondrial pellet was immediately lysed in a buffer containing 1% SDS, 63 mM Tris, pH 6.8. In order to concentrate samples, cytosolic proteins of the supernatant were then precipitated by adding an equal volume of acetone supplemented with acetic acid (10%, v/v) for 1 h at 4°C . The precipitates were centrifuged at $12,000 \times g$ for 15 min at 4°C before the proteins were re-dissolved in the lysis buffer. Mitochondrial and cytosolic proteins were then used for western blotting as described above.

2.9. Mitochondrial membrane potential assessment

For mitochondrial membrane potential measurement, the 5,5',6,6',7 tetrachloro-1,1',4,4'-tetraethylbenzimidazolyl carbocyaniniodide (JC-1) cationic dye was used. It accumulates and aggregates in a concentration-dependent manner in polarized mitochondria, emitting a red fluorescence (590 nm) after excitation at 480 nm. Conversely, in depolarized mitochondria, the dye concentration is weak and it stays as monomers emitting a green fluorescence (530 nm) after excitation at 480 nm. A 250×10^3 cells were suspended in 3 ml of PBS supplemented with $1 \mu\text{M}$

JC-1 and incubated for 30 min at 37°C before being harvested and re-suspended in 500 μl of PBS. A volume of 150 μl of the cell suspension were then transferred into wells of 96-well plates (Greiner) and the fluorescence was read by using the spectra Max fluorescence GEMINI microplate reader as described above (excitation at 480 nm and detection at 530 and 590 nm, respectively for green and red). The mitochondrial membrane potential was assessed as the red/green ratio emission after excitation at 480 nm.

3. Results

3.1. PBR ligands are toxic for both SK-N-BE neuroblastoma cells and Jurkat cells

First, we assessed cultured SK-N-BE neuroblastoma and wt-Jurkat lymphoma cells for PBR expression, both at the transcript and the protein levels (Fig. 1A and B). mRNAs extracted from both cell lines, as well as from LN18 glioma cells used as positive controls, were subjected to RT-PCR (Fig. 1A) and yielded a signal for LN18 and SK-N-BE cells only, consistent with the reported absence of PBR expression in Jurkat cells [39]. These results were confirmed by immunoblotting. Indeed, as shown in Fig. 1B, PBR

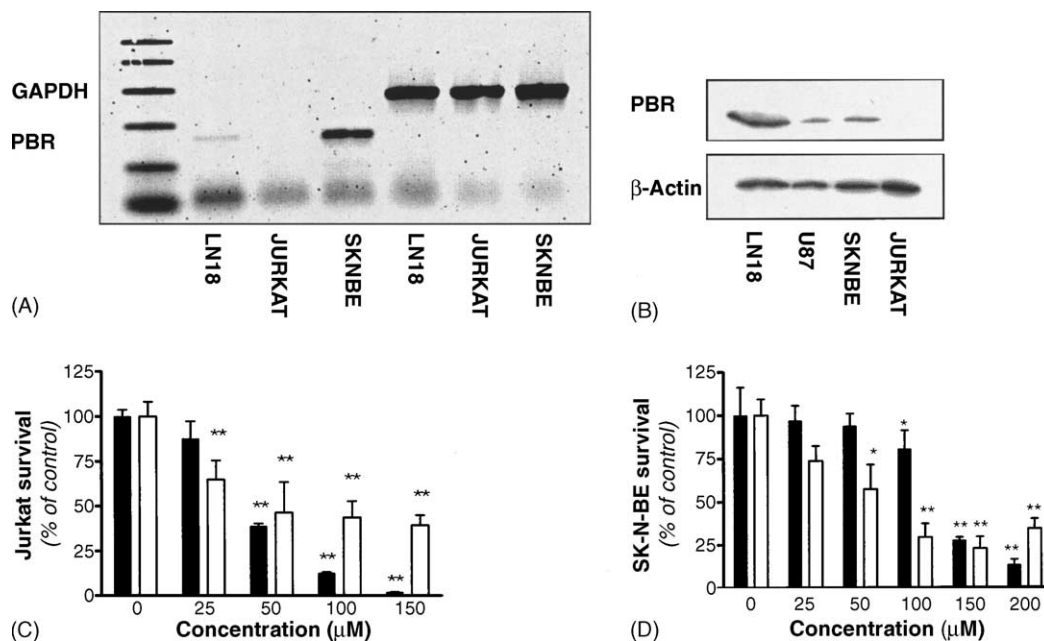


Fig. 1. PBR ligands are toxic for both PBR-expressing and PBR-lacking cells. (A) Total mRNAs extracted from LN18 glioma cells, wild-type lymphoid Jurkat cells and SK-N-BE neuroblastoma cells were subjected to RT-PCR analysis. Amplification of GAPDH mRNAs was used as a positive control. (B) Western blotting detection of the PBR by using the 8D7 antibody. The single 18 kDa band corresponds to the. Western blotting of β -actin was used as a positive control. (C) The toxicity of Ro 5-4864 (black bars) and of FGIN 1-27 (open bars) was assessed in wt-Jurkat cells. The cellular survival was determined by the live/dead ratio after 24 h in the presence of the PBR ligands. Bars represent the live/dead ratio expressed as the percentage of the same ratio in controls (mean \pm S.D., $n = 4$ in this experiment which is representative of three independent). $**P < 0.01$, using ANOVA followed by multiple Dunnett's post-test. (D) SK-N-BE cells were grown for 24 h in the presence of increasing concentrations of Ro 5-4864 (black bars) or FGIN 1-27 (open bars). The survival was assessed by using the MTT assay and expressed as a percentage of the survival in control conditions, i.e. without any drug (mean \pm S.D., $n = 4$ in this experiment which is representative of three independent). $*P < 0.05$, $**P < 0.01$, using ANOVA followed by multiple Dunnett's post-test.

proteins are present in SK-N-BE neuroblastoma cells and in two glioma cell lines (LN-18 and U-87) while completely absent in Jurkat cells.

Thereafter, the effect of two chemically unrelated PBR ligands, Ro 5-4864 and FGIN-1-27, on the survival of both SK-N-BE and Jurkat cells was assessed. Increasing concentrations of Ro 5-4864 and of FGIN-1-27 induced a dose-dependent toxicity towards Jurkat cells (Fig. 1C) as well as SK-N-BE cells (Fig. 1D). In both cell types, FGIN-1-27 (light bars) was slightly more potent than Ro 5-4864 (black bars) in inducing cell death. Indeed, its IC_{50} was $38 \pm 7 \mu\text{M}$ compared to $133.7 \pm 11 \mu\text{M}$ for Ro 5-4864 in SK-N-BE ($n = 6$; $P < 0.0001$, Student t -test) and $21.5 \pm 1.5 \mu\text{M}$ compared to $43 \pm 3.6 \mu\text{M}$ for Ro 5-4864 in Jurkat cells ($n = 4$; $P < 0.0001$, Student t -test). On the other hand, and again in both cell types, Ro 5-4864 displayed a higher efficacy in killing cells, yielding at its higher concentration a maximal toxicity (measured as percent of cell survival) of $13.4 \pm 3\%$ compared to $34.4 \pm 11.2\%$ for FGIN-1-27 in SK-N-BE ($n = 6$; $P < 0.05$, Student t -test) and of $2 \pm 0.06\%$ compared to $39.5 \pm 5.6\%$ for FGIN-1-27 in Jurkat cells ($n = 4$; $P < 0.001$, Student t -test).

3.2. Ro 5-4864-induced cell death has apoptotic features in Jurkat cells but not in SK-N-BE cells

Due to its higher toxicity efficacy, Ro 5-4864 was chosen to characterize the biochemical pathways of SK-N-BE and Jurkat cell death.

As a first step in this characterization, the pattern of DNA fragmentation and the cleavage of PARP were studied to differentiate between apoptosis and necrosis. As shown in Fig. 2, Ro 5-4864-induced Jurkat cell death has the hallmark of apoptosis. Firstly, treatment with $150 \mu\text{M}$ Ro 5-4864 for 24 h induced a 2.21-fold increase in the proportion of Jurkat cells presenting an apoptotic DNA fragmentation as assessed by the TUNEL labeling (Fig. 2A; $P < 0.001$; Student t -test). Secondly, further analysis of dying Jurkat cells by DNA gel electrophoresis confirmed that $150 \mu\text{M}$ Ro 5-4864-induced an internucleosomal DNA fragmentation as demonstrated by the presence of a typical laddering indicating a low molecular weight DNA fragmentation (Fig. 2C). Thirdly, the apoptotic nature of Ro 5-4864-induced Jurkat cell death was confirmed by the apparition of a 85 kDa cleaved fragment of PARP 16 h after the beginning of the treatment (Fig. 2E). Such a PARP cleavage is known to occur both in vivo and in vitro when caspase-3 is activated [40]. On the opposite, the cell death induced by Ro 5-4864 in SK-N-BE cells differed strikingly from that observed in Jurkat cells. No significant increase in the proportion of TUNEL-labeled SK-N-BE cells could be observed after a 24 h exposure to $150 \mu\text{M}$ Ro 5-4864 (Fig. 2B). Consistent with the absence of TUNEL labeling, no laddering of DNA extracted from dying SK-N-BE cells could be noticed (Fig. 2D). Finally,

we observed that PARP cleavage during the dying process of SK-N-BE cells exposed to Ro 5-4864 ($150 \mu\text{M}$ for various times between 0 and 24 h) resulted in the production of a lower molecular weight PARP cleaved fragment than in Jurkat cells (25–30 compared to 85 kDa; Fig. 2F), which may reflect the activation of other proteases unrelated to caspases like calpain or cathepsins [40].

To get sure that caspases were indeed involved in Ro 5-4864-induced Jurkat but not SK-N-BE cell death, their activation was assessed after increasing times by immunoblotting (Fig. 3). In Jurkat cells, Ro 5-4864-induced an activation of the initiating caspase-8, as shown by the decrease in the intensity of the pro-enzyme and the appearance of the cleaved fragment p40. The caspase-3 and -9 were concomitantly activated as depicted by a reduction of their pro-enzyme intensity over the time (left part of Fig. 3). This activation became apparent from 16 h after the beginning of exposure to $150 \mu\text{M}$ Ro 5-4864, which also corresponds to the apparition of the PARP cleavage. Conversely, no detectable activation of the effector caspase-3 could be observed in treated SK-N-BE cells, even after 24 h of exposure to $150 \mu\text{M}$ Ro 5-4864 (right part of Fig. 3), further indicating that Ro 5-4864 is unlikely to induce an apoptotic death of these cells. Moreover, in SK-N-BE cells, no signal for pro-caspase-8 and -9 could be detected, as already observed in previous works with neuroblastoma [41].

If caspase activation is a necessary step in the biochemical pathway leading to the death of Ro 5-4864-treated Jurkat cells, caspase inhibitors should provide some degree of protection. Indeed, co-incubation of Jurkat cells with $20 \mu\text{M}$ Boc-D-FMK (a pancaspase inhibitor), Ac-DEVD-CHO (a caspase-3 inhibitor) or Z-LETD-FMK (a caspase-8 inhibitor) all resulted in a significant reduction of $150 \mu\text{M}$ Ro 5-4864-induced apoptosis (Fig. 4A). No protection was however observed with Z-LEHD-FMK, a caspase-9 inhibitor. The protective effect of Z-LETD-FMK suggests that caspase-8 could be a crucial step leading to Jurkat cell apoptosis upon Ro 5-4864 treatment. To further test this hypothesis, we first measured the laddering of Jurkat cell DNA in the presence of Ro 5-4864 alone or in combination with Z-LETD-FMK. As shown in Fig. 4C, the oligonucleosomal DNA fragmentation observed with Ro 5-4864 alone completely disappears in the presence of Z-LETD-FMK. We then looked for the activation of the caspase cascade in the presence of the caspase-8 inhibitor and observed (Fig. 4B) that Z-LETD-FMK not only inhibits caspase-8 activation, as measured by a lower decrease in pro-caspase-8 and a lower increase in its cleaved fragment p40, but also diminish the activation of downstream events, i.e. it decreases the disappearance of pro-caspase-3 and -9, as well as the cleavage of PARP (Fig. 4B).

On the other hand, and consistent with the absence of any caspase activation in SK-N-BE cells treated with $150 \mu\text{M}$ Ro 5-4864, no protection was observed with

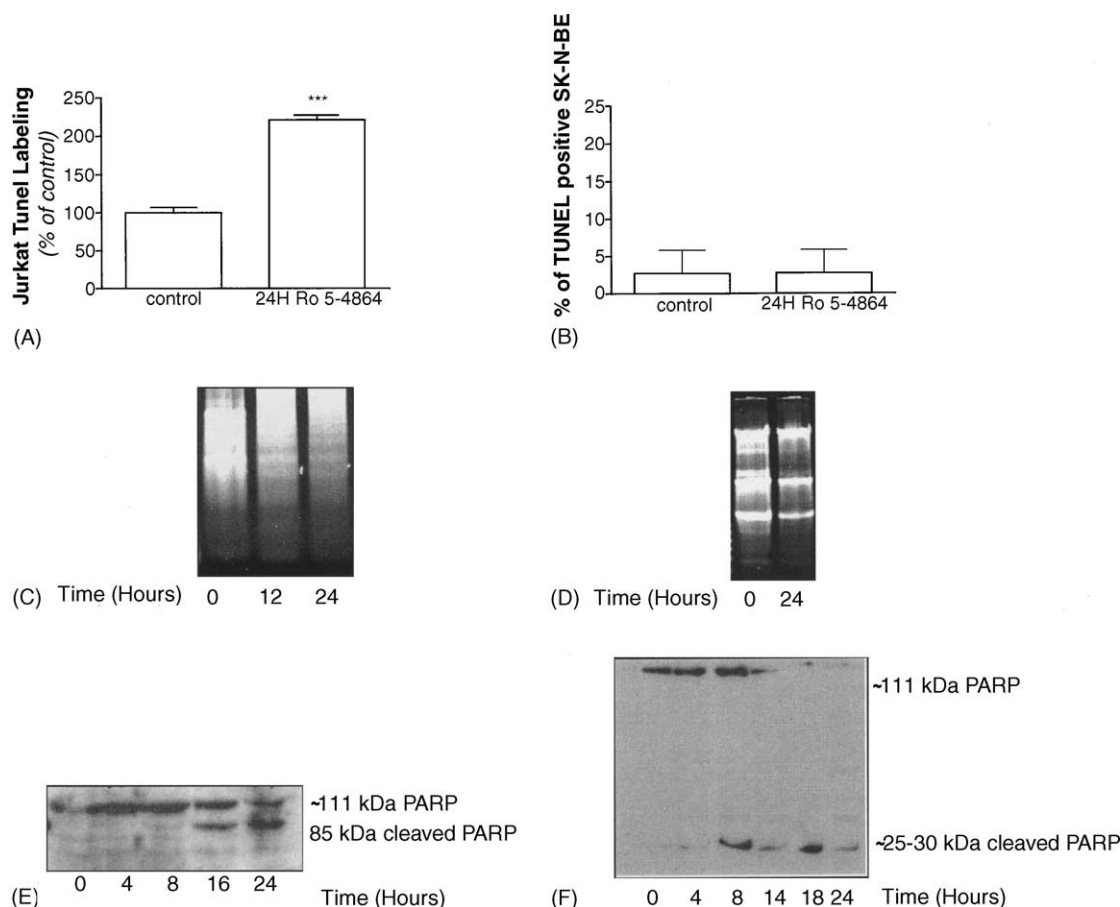


Fig. 2. Ro 5-4864-induced cell death is apoptotic in Jurkat cells while necrotic in SK-N-BE cells. (A) TUNEL labeling was performed in wt-Jurkat cells after 24 h of exposure to 150 μ M Ro 5-4864. Bars represent the fluorescence intensity of the cell suspension (measured with a fluorescence microplate reader, see Section 2) expressed as percent of the same fluorescence in controls (mean \pm S.D., $n = 3$ different conditions in this representative experiment). *** $P < 0.001$, Student t -test. (B) SK-N-BE cells were exposed to 150 μ M Ro 5-4864 during 24 h and subsequently subjected to TUNEL labeling. Marked cells were then counted under a fluorescence microscope. Bars correspond to the percentage of TUNEL positive cells in each condition (mean \pm S.D., $n = 4$ different fields per condition in this experiment representative of three independent). (C and D) Total DNA extracts from Jurkat cells (C) and from SK-N-BE cells (D) exposed to 150 μ M Ro 5-4864 during 12–24 h were subjected to agarose gel electrophoresis. (E and F) 30 μ g of Jurkat (E) and of SK-N-BE (F) cell lysates obtained after the indicated time periods (h) following exposure to 150 μ M Ro 5-4864 were subjected to SDS-PAGE electrophoresis and subsequently immunoblotted with anti-PARP antibodies.

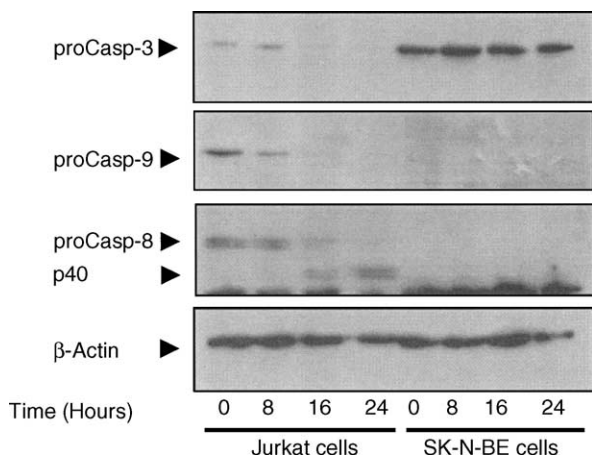


Fig. 3. Ro 5-4864 activates caspases in Jurkat cells but not in SK-N-BE cells. Jurkat and SK-N-BE cells were incubated with 150 μ M Ro 5-4864 for the indicated times. The activities of caspase-3, -8 and -9 were assessed by immunoblotting.

any of the tested caspase inhibitors towards the toxicity of Ro 5-4864 in these cultures (Fig. 4D).

3.3. Ro 5-4864-induced cell death is associated with a mitochondrial impairment which occurs early in SK-N-BE but late in Jurkat cells

As already mentioned in the introduction, mitochondrion impairment occurs frequently in the course of cell death. However, mitochondrion impairment-related events, such as cytochrome *c* release or $\Delta\psi_m$ loss can be either the hallmark of a triggering role of the mitochondrion in the cell death process (necrotic as well as apoptotic) or a consequence of an apoptotic cascade initiated elsewhere, thereby acting sometimes as an enhancing loop [42]. Therefore, and in order to look

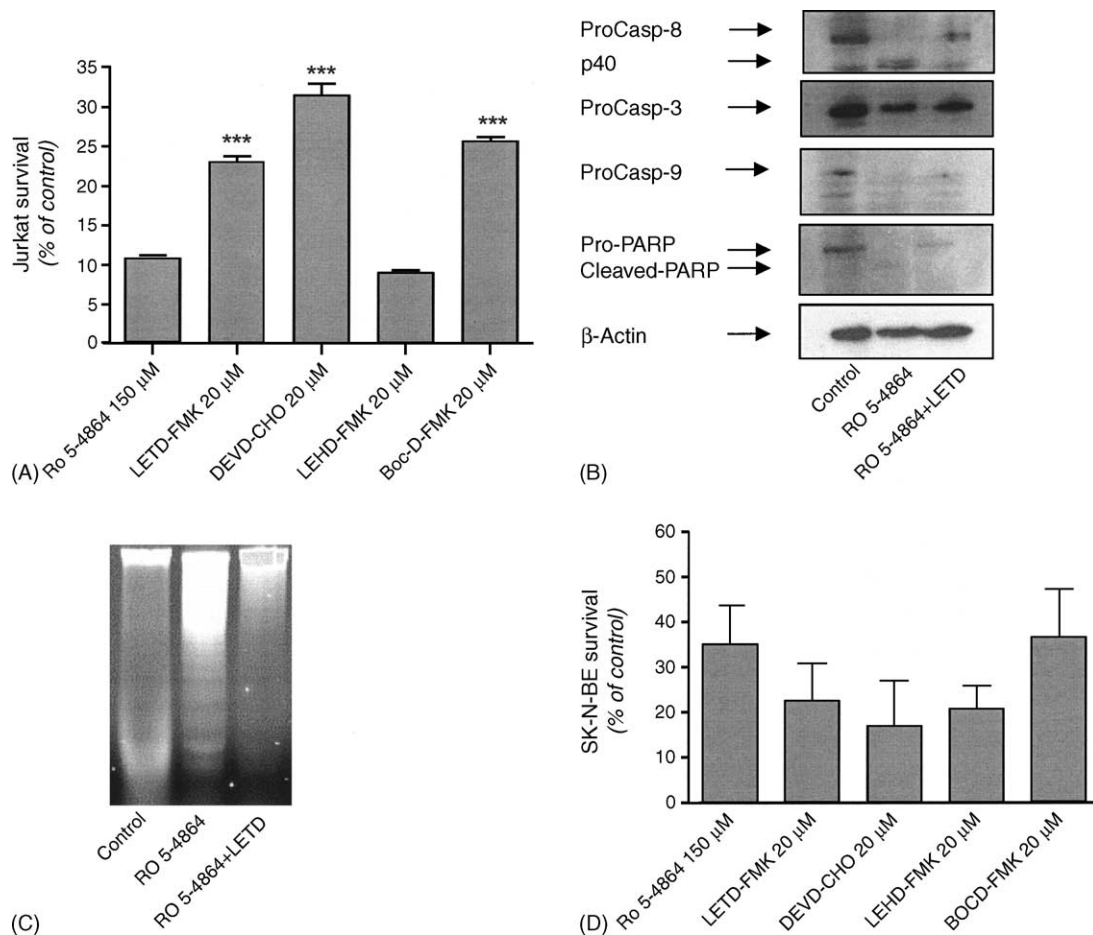


Fig. 4. Caspase inhibitors protect Jurkat but not SK-N-BE cells against Ro 5-4864-induced toxicity. (A) Live/dead assay for assessment of Jurkat cell survival after a 24 h exposure to 150 μ M Ro 5-4864 alone or combined with a caspase inhibitor: LETD-FMK (caspase-8 inhibitor), DEVD-CHO (caspase-3 inhibitor), LEHD-FMK (caspase-9 inhibitor) and BOC-D-FMK (pan-caspase inhibitor). Bars represent the live/dead ratio expressed in percent of controls, i.e. without any added drugs (mean \pm S.D., $n = 3$ replicate conditions in this experiment which is representative of three independent). *** $P < 0.001$ by using ANOVA followed by Dunnett's post-tests. (B) Whole cell lysates of Jurkat cells were obtained in control conditions (lane 1), after 24 h of exposure to 150 μ M Ro 5-4864 alone (lane 2) or together with 20 μ M LETD-FMK (lane 3). Caspase activation and PARP cleavage were then assessed by immunoblotting. (C) Whole-cell DNA extracts from control Jurkat cells (lane 1), Jurkat cells exposed for 24 h to 150 μ M Ro 5-4864 (lane 2) and Jurkat cells treated for 24 h with 150 μ M Ro 5-4864 + 20 μ M LETD-FMK (lane 3) were submitted to agarose gel electrophoresis. (D) SK-N-BE cell viability was assessed by using the MTT assay after 24 h of exposure to 150 μ M Ro 5-4864 either alone or together with 20 μ M of caspase inhibitors (see (A) above). Results are expressed as percent of MTT transformation in controls, i.e. without added Ro 5-4864 (mean \pm S.D., $n = 6$ replicate wells in this experiment which is representative of three independent).

for a mitochondrial impairment in PBR ligand-induced cell death, we looked for such mitochondrial changes in a time-related manner.

In that respect, we show using immunoblotting that Ro 5-4864 induces a time-dependent cytochrome *c* release from the mitochondria into the cytosol both in Jurkat (Fig. 5A) and in SK-N-BE cells (Fig. 5B). This release occurred however earlier in SK-N-BE than in Jurkat cells (12 h versus 16 h, respectively).

To further characterize the mechanism of Ro 5-4864-induced cytochrome *c* release, the $\Delta\psi_m$ was monitored during exposure to 150 μ M Ro 5-4864 by using the JC-1 technique. In Jurkat cells, a significant decrease in the JC-1590:530 nm ratio emission, which reflects a loss of $\Delta\psi_m$, was observed from 18 h after the addition of Ro 5-4864 (Fig. 5C). A similar $\Delta\psi_m$ loss was also measured in treated SK-N-BE cells (Fig. 5D). However in these cells, the

mitochondrial depolarization became apparent much earlier than in Jurkat cells, i.e. from 4 to 8 h after the beginning of exposure to Ro 5-4864. Taken together, these results demonstrate that mitochondria-related events following Ro 5-4864 treatment occur earlier in SK-N-BE than in Jurkat cells.

Since a loss of $\Delta\psi_m$ usually reflects an opening of the mitochondrial permeability transition pore (mPTP), we addressed the significance of such an opening in the Ro 5-4864-induced cell death process. For this purpose, the potential protective effects of two mPTP inhibitors, i.e. cyclosporine A (CsA) and Bongkrekic acid (BA), were assessed in both Jurkat and SK-N-BE cells. Fig. 5E and F illustrates that neither 5 μ M CsA nor 50 μ M BA protect against the toxicity of 150 μ M Ro 5-4864 measured in Jurkat cells using the live/dead assay and with the MTT assay in SK-N-BE cells (see Section 2).

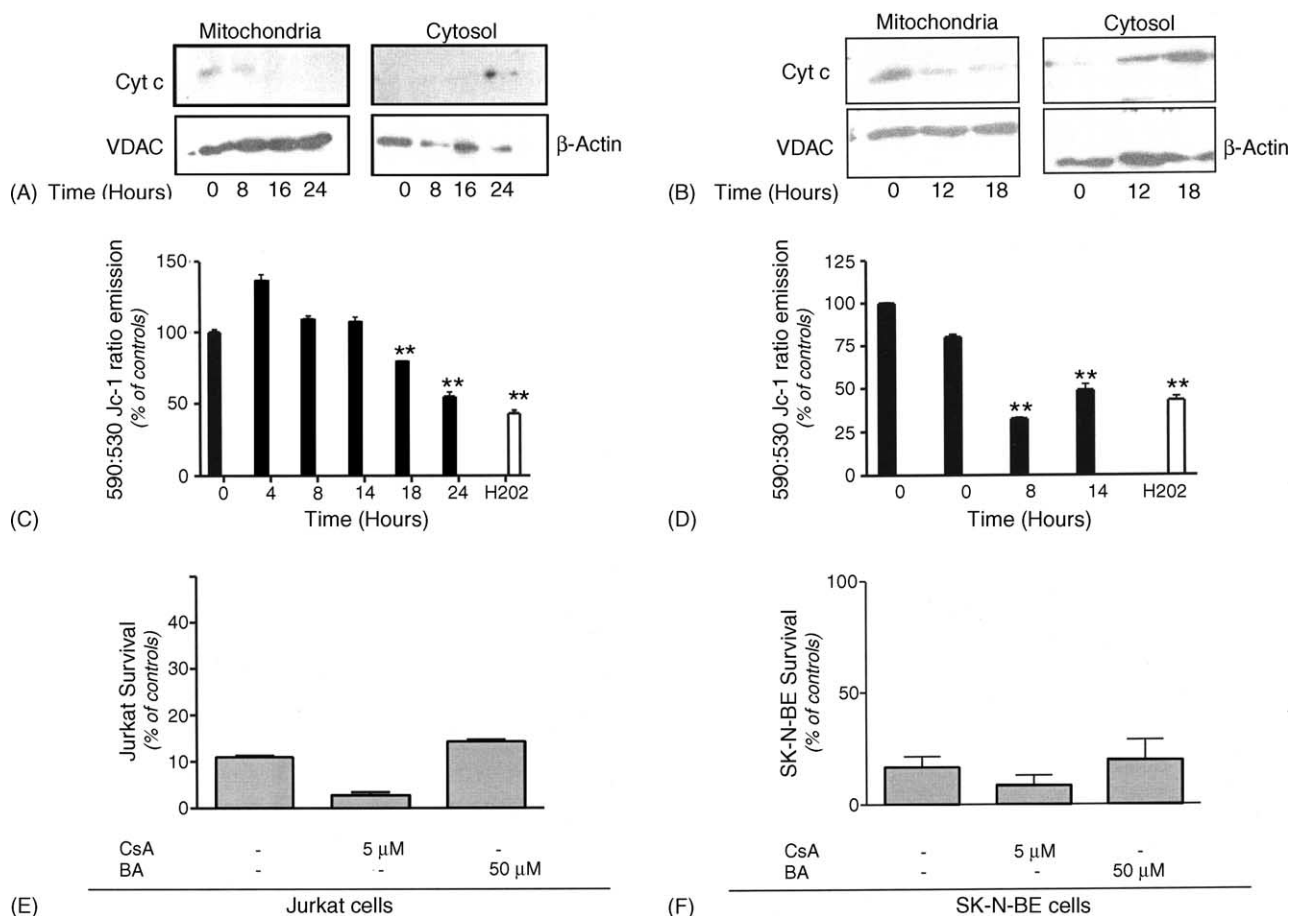


Fig. 5. Ro 5-4864 induces a cytosolic release of cytochrome *c* and a mitochondrial membrane depolarization which occur early in SK-N-BE cells and late in Jurkat cells. (A) The subcellular distribution of the cytochrome *c* in Jurkat cells was studied during exposure to 150 μ M Ro 5-4864 by cellular fractionation and subsequent immunoblotting. Incubation of the same blots with anti-VDAC and anti- β -actin antibodies was used as a control of cell fractionation. (B) Similar immunoblots were performed in SK-N-BE cells exposed to 150 μ M Ro 5-4864. (C) The mitochondrial membrane potential ($\Delta\psi_m$) was monitored in Jurkat cells by using the JC-1 technique during a time-course of exposure to 150 μ M Ro 5-4864. Bars represent the 590 nm:530 nm fluorescence ratio emission expressed as percent of the same ratio in controls, (mean \pm S.D., $n = 3$ replicate conditions in this experiment which is representative of three independent). Exposure of Jurkat cells to 20 μ M H₂O₂ during 20 min was used as a positive control. $**P < 0.01$ using ANOVA followed by Dunnett's *post*-tests. (D) A similar $\Delta\psi_m$ monitoring was performed in SK-N-BE cells treated with 150 μ M Ro 5-4864. (E) The effect of two mPTP inhibitors, i.e. cyclosporine A (CsA) and Bongkrekic acid (BA), on the toxicity induced by a 24 h exposure to 150 μ M Ro 5-4864 in Jurkat cells was assessed by using the live/dead assay. Bars represent mean live/dead ratios expressed as percent of the same ratio in controls, i.e. without added Ro 5-4864 (mean \pm S.D., $n = 4$ replicate wells in this experiment which is representative of three independent). (F) As for (E), the effects of BA and CsA on Ro 5-4864-induced toxicity in SK-N-BE cells were assessed by using the MTT assay. Bars represent the mean survival expressed as percent of controls; i.e. without Ro 5-4864 added (mean \pm S.D., $n = 6$ replicate wells in this representative experiment).

3.4. Expression of PBR in Jurkat cells do not switch Ro 5-4864-induced cell death into necrosis

From the results presented so far, it could appear that, since PBR ligands kill both PBR-containing and PBR-lacking cells, PBR would hardly play a role in PBR ligand-induced death. However, we also report that Ro 5-4864-induced Jurkat cell death has apoptotic features while, in SK-N-BE, the Ro 5-4864 toxicity seems rather necrotic. Since PBR takes part in the mPTP and may thus regulate the apoptosis/necrosis switch [27], we studied the features of Ro 5-4864-induced toxicity in Jurkat cells stably transfected with the PBR.

The results are presented in Fig. 6 and can be summarized as follows. Firstly, transfected Jurkat cells express

indeed the PBR both at the transcript (data not shown) and at the protein levels (Fig. 6A), although less intensely than SK-N-BE cells. Secondly, the dose-dependent toxicity of Ro 5-4864 on PBR-transfected Jurkat cells (Fig. 6B) was not significantly different from the one obtained on wild-type Jurkat cells; both the potency ($IC_{50} = 88.2 \pm 20.0 \mu$ M, $n = 3$) and the efficacy (maximal toxicity = $8.6 \pm 0.2\%$; $n = 3$ of control cell survival) were in the same range order. Thirdly, the DNA cleavage that occurred during Ro 5-4864-induced death of PBR-transfected Jurkat cells had apoptotic features as demonstrated by the increase in TUNEL labeling (Fig. 6C) and by the laddering of the low molecular weight fragments (Fig. 6D). Finally, Ro 5-4864 also induced an activation of caspase-3, -8 and -9 in PBR-transfected Jurkat cells,

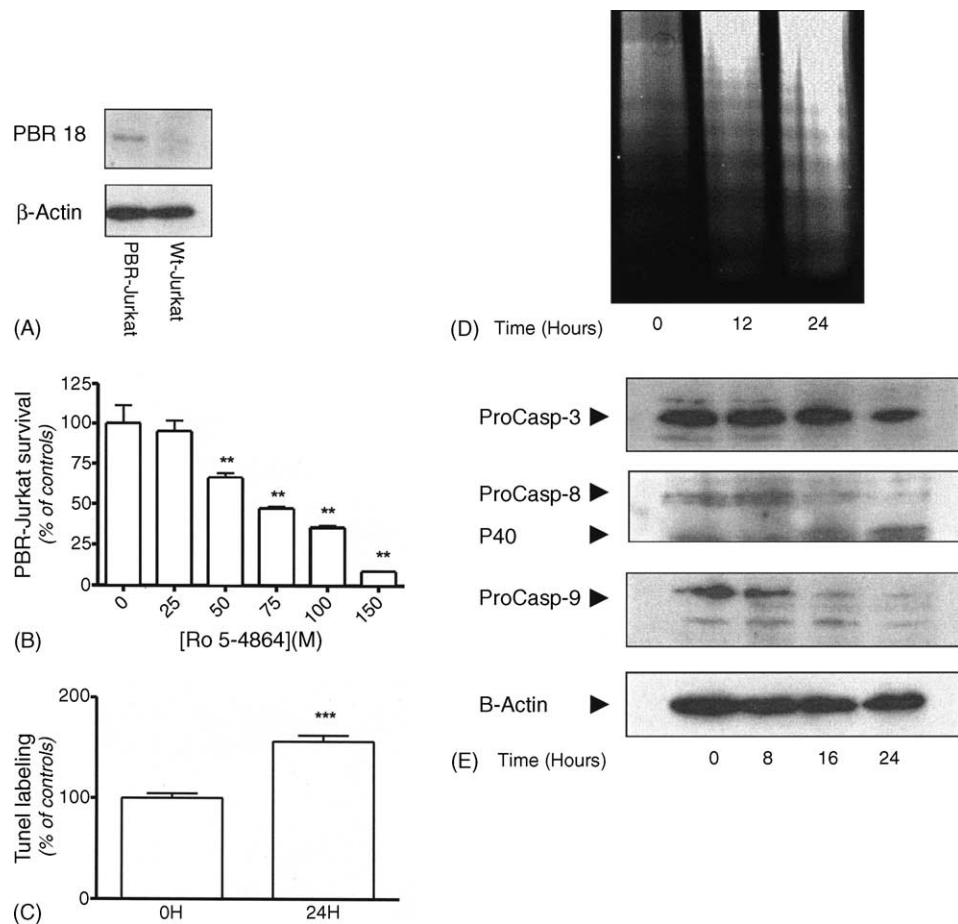


Fig. 6. Expression of PBR in Jurkat cells does not convert Ro 5-4864-induced apoptosis into necrosis. (A) PBR expression was assessed by immunoblotting in PBR-transfected Jurkat cells and wild-type Jurkat cells. (B) The effect of Ro 5-4864 on PBR-transfected Jurkat cells was assessed after 24 h by the live/dead assay. Bars represent the survival (live/dead ratio) expressed as percent of the same ratio in controls (mean \pm S.D., $n = 4$ in this experiment which is representative of three independent). $^{**}P < 0.01$ using ANOVA followed by Dunnett's post-tests. (C and D) TUNEL labeling (C) and DNA agarose gel electrophoresis (D) were performed on PBR-transfected Jurkat cells treated for 24 h with 150 μ M Ro 5-4864. (E) The pattern of caspase activation in PBR-transfected Jurkat cells along a time-course of exposure to 150 μ M Ro 5-4864 was studied by immunoblotting (as in Fig. 3).

further demonstrating that it triggers apoptosis, as in wild-type Jurkat cells.

4. Discussion

The present study demonstrates that micromolar concentrations of two chemically unrelated PBR ligands, i.e. Ro 5-4864 and FGIN-1-27, are toxic for both PBR-expressing SK-N-BE neuroblastoma and PBR-deficient Jurkat lymphoma cells. Moreover, the molecular pathways leading to Ro 5-4864-induced cell death differ strikingly between the two types of cell, being apoptotic in Jurkat while necrotic in SK-N-BE cells. Nevertheless, expressing PBR in Jurkat cells does not modify the features of Ro 5-4864-induced cell death.

To our knowledge, this study brings the first conclusive evidence that PBR ligand-induced cell death is unrelated to their PBR-binding property. Indeed, since Jurkat cells, which completely lack PBR expression, are as sensitive as SK-N-BE or PBR-transfected Jurkat cells to PBR ligand

toxicity, any PBR involvement in PBR ligand-induced death seems definitely ruled out. The relationship between PBR ligand toxicity and their binding to PBR has already been questioned in several studies where the concentration range needed to achieve a toxic effect was always two or three orders of magnitude higher than the affinity of PBR ligands for their receptor [8–12]. Furthermore, a similar debate existed about the effect of PBR ligands on cell proliferation [43], and it has just been demonstrated that such a property was independent of their ability to bind PBR [44]. Consistently with previous findings related to their toxicity, in this study, we have observed that the toxic concentrations of PBR ligands were in the 10–100 μ M range.

The cellular events observed during Ro 5-4864-induced cell death provide further evidence favouring a PBR-unrelated hypothesis. Indeed, in PBR-deficient Jurkat cells, Ro 5-4864 had apoptotic features as demonstrated by the presence of an internucleosomal DNA fragmentation [45] and a PARP cleavage into an 85 kDa fragment [40]. Moreover, it was associated with an activation of caspases, key

players of the apoptotic machinery [46]. Regarding the mitochondrial alterations induced by Ro 5-4864 in Jurkat cells, both the $\Delta\psi_m$ loss and the cytosolic release of the cytochrome *c* occur late (18–24 h after the beginning of treatment), in particular after the first signs of caspase activation and apoptotic DNA fragmentation (12–16 h). They might therefore rather be considered as secondary mitochondrial changes, as described in many apoptotic processes where mitochondria act as executioners [32]. Active caspases can indeed trigger such mitochondrial changes either through the caspase-8-mediated bid cleavage [47] or via caspase-3-induced alterations in electron transport complexes [33]. Interestingly, the activation of caspase-8 seems crucial in our model as underlined by the protection afforded by Z-LETD-FMK, a specific caspase-8 inhibitor. Our observed lack of sensitivity of Ro 5-4864-induced cell death to CsA and BA also fits well with a secondary mitochondrial permeabilisation. Indeed, both caspase-3 and tBid-mediated $\Delta\psi_m$ losses are described as mPTP-independent [33,47].

The features of Ro 5-4864-induced SK-N-BE cell death appear strikingly different. Indeed, no apoptotic DNA cleavage and no caspase activation were detected, hence suggesting more a necrotic process. Furthermore, the mitochondrial membrane depolarisation and the cytosolic cytochrome *c* release occurred earlier than in Jurkat cells. This could reflect a massive mPTP opening and explain the necrotic features of subsequent cell death [30]. However, mPTP inhibitors failed to protect against Ro 5-4864-induced SK-N-BE death. This discrepancy could only be explained by the occurrence of an unregulated [48] or aberrantly regulated mPTP [49] as already described following PK11195 exposure. This hypothesis would however need further experiments to be confirmed.

One could also argue that such differences in death features should be attributed to the abundant expression of the PBR in SK-N-BE cells. Strong evidence indeed exist in favour of a regulatory role of the PBR in mPTP opening [50,51]. Nanomolar concentrations of PK11195 are moreover able to trigger an increase in ROS production [52], which in turn can lead to an mPTP opening [53]. However, PBR-expressing Jurkat cells undergo an apoptotic cell death after exposure to Ro 5-4864, similarly to the corresponding wild types. This latter observation virtually excludes any role of the PBR in the Ro 5-4864-induced cell death.

A more likely explanation of our observed differences between the cell death biochemical cascades triggered by PBR ligands in Jurkat versus SK-N-BE cells could rather lie within their pattern of caspase expression. SK-N-BE were indeed found not to express caspase-8 and caspase-9. Such caspase deficiencies were already described for other neuroblastoma cell lines [41,54]. Interestingly, caspase-8 which seems to be a key player in the Ro 5-4864-induced Jurkat cells apoptosis, has also been implicated in the apoptosis/necrosis switch [55]. In that respect, Fas-induced

fibrosarcoma cells apoptosis has indeed been shown to be converted into necrosis in the presence of a broad spectrum caspase inhibitor [56]. Moreover, Fas-induced necrosis was reported in a caspase-8 deficient Jurkat cell line [57].

The abundant expression of PBR in cancer cells and the correlation of its expression level with tumor malignancy, together with the cytotoxic properties of PBR ligands for malignant cells suggested that PBR ligands might be promising drugs in the field of cancer. Here, on the one hand, we report the absence of any relationship between the cytotoxicity of some PBR ligands and their PBR-binding property. Such findings should restrict the development of new cytotoxic drugs exclusively based upon their PBR-binding profile, but rather direct future research to an understanding of the actual primary target that mediates their pro-apoptotic/necrotic effect. This target could indeed be of essential interest regarding the development of new chemotherapeutic agents. On the other hand, we provide further support in the development of drugs similar to existing PBR ligands since we show that they are even effective on reputed chemoresistant cells such as caspase-deficient neuroblastoma. Even more, we would encourage not to limit their use to PBR-expressing tumors.

Acknowledgements

This work was supported by the *Fonds National de la Recherche Scientifique* (FNRS), the *Fondation Médicale Reine Elisabeth* and the *Fondation Rahier*. G. Hans is research fellow of the FNRS. B. Rogister is senior research associate of the FNRS, S. Belachew and B. Malgrange are research associates of the FNRS. We also would like to thank the *Fondation Médicale Reine Elisabeth* and the *Fondation Rahier*. We are also very grateful to Patricia Gengoux and Arlette Brose for their technical expertise.

References

- [1] Anholt RR, Pedersen PL, De Souza EB, Snyder SH. The peripheral-type benzodiazepine receptor localization to the mitochondrial outer membrane. *J Biol Chem* 1986;261:576–83.
- [2] Krueger KE. Molecular and functional properties of mitochondrial benzodiazepine receptors. *Biochim Biophys Acta* 1995;1241:453–70.
- [3] Bribes E, Carriere D, Goubet C, Galiegue S, Casellas P, Simony-Lafontaine J. Immunohistochemical assessment of the peripheral benzodiazepine receptor in human tissues. *J Histochem Cytochem* 2004;52:19–28.
- [4] Beurdeley-Thomas A, Miccoli L, Oudard S, Dutrillaux B, Poupon MF. The peripheral benzodiazepine receptors: a review. *J Neurooncol* 2000;46:45–56.
- [5] Casellas P, Galiegue S, Basile AS. Peripheral benzodiazepine receptors and mitochondrial function. *Neurochem Int* 2002;40:475–86.
- [6] Galiegue S, Tinel N, Casellas P. The peripheral benzodiazepine receptor: a promising therapeutic drug target. *Curr Med Chem* 2003;10:1563–72.

- [7] Gavish M, Bachman I, Shoukrun R, Katz Y, Veenman L, Weisinger G, et al. Enigma of the peripheral benzodiazepine receptor. *Pharmacol Rev* 1999;51:629–50.
- [8] Sutter AP, Maaser K, Hopfner M, Barthel B, Grabowski P, Faiss S, et al. Specific ligands of the peripheral benzodiazepine receptor induce apoptosis and cell cycle arrest in human esophageal cancer cells. *Int J Cancer* 2002;102:318–27.
- [9] Sutter AP, Maaser K, Barthel B, Scherubl H. Ligands of the peripheral benzodiazepine receptor induce apoptosis and cell cycle arrest in oesophageal cancer cells: involvement of the p38MAPK signalling pathway. *Br J Cancer* 2003;89:564–72.
- [10] Sutter AP, Maaser K, Gerst B, Krahn A, Zeitz M, Scherubl H. Enhancement of peripheral benzodiazepine receptor ligand-induced apoptosis and cell cycle arrest of esophageal cancer cells by simultaneous inhibition of MAPK/ERK kinase. *Biochem Pharmacol* 2004;67:1701–10.
- [11] Decaudin D, Castedo M, Nemati F, Beurdeley-Thomas A, De Pinieux G, Caron A, et al. Peripheral benzodiazepine receptor ligands reverse apoptosis resistance of cancer cells in vitro and in vivo. *Cancer Res* 2002;62:1388–93.
- [12] Hirsch T, Decaudin D, Susin SA, Marchetti P, Larochette N, Resche-Rigon M, et al. PK11195, a ligand of the mitochondrial benzodiazepine receptor, facilitates the induction of apoptosis and reverses Bcl-2-mediated cytoprotection. *Exp Cell Res* 1998;241:426–34.
- [13] Miettinen H, Kononen J, Haapasalo H, Helen P, Sallinen P, Harjuntausta T, et al. Expression of peripheral-type benzodiazepine receptor and diazepam binding inhibitor in human astrocytomas: relationship to cell proliferation. *Cancer Res* 1995;55:2691–5.
- [14] Cornu P, Benavides J, Scatton B, Hauw JJ, Philippon J. Increase in omega 3 (peripheral-type benzodiazepine) binding site densities in different types of human brain tumours. A quantitative autoradiography study. *Acta Neurochir (Wien)* 1992;119:146–52.
- [15] Maaser K, Grabowski P, Sutter AP, Hopfner M, Foss HD, Stein H, et al. Overexpression of the peripheral benzodiazepine receptor is a relevant prognostic factor in stage III colorectal cancer. *Clin Cancer Res* 2002;8:3205–9.
- [16] Hardwick M, Fertikh D, Culty M, Li H, Vidic B, Papadopoulos V. Peripheral-type benzodiazepine receptor (PBR) in human breast cancer: correlation of breast cancer cell aggressive phenotype with PBR expression, nuclear localization, and PBR-mediated cell proliferation and nuclear transport of cholesterol. *Cancer Res* 1999;59:831–42.
- [17] Hardwick M, Rone J, Han Z, Haddad B, Papadopoulos V. Peripheral-type benzodiazepine receptor levels correlate with the ability of human breast cancer MDA-MB-231 cell line to grow in SCID mice. *Int J Cancer* 2001;94:322–7.
- [18] Debatin KM, Poncet D, Kroemer G. Chemotherapy: targeting the mitochondrial cell death pathway. *Oncogene* 2002;21:8786–803.
- [19] Maaser K, Hopfner M, Jansen A, Weisinger G, Gavish M, Kozikowski AP, et al. Specific ligands of the peripheral benzodiazepine receptor induce apoptosis and cell cycle arrest in human colorectal cancer cells. *Br J Cancer* 2001;85:1771–80.
- [20] Chelli B, Lena A, Vanacore R, Pozzo ED, Costa B, Rossi L, et al. Peripheral benzodiazepine receptor ligands: mitochondrial transmembrane potential depolarization and apoptosis induction in rat C6 glioma cells. *Biochem Pharmacol* 2004;68:125–34.
- [21] Zisterer DM, Campiani G, Nacci V, Williams DC. Pyrrolo-1,5-benzoxazepines induce apoptosis in HL-60, Jurkat, and Hut-78 cells: a new class of apoptotic agents. *J Pharmacol Exp Ther* 2000;293:48–59.
- [22] Fischer R, Schmitt M, Bode JG, Haussinger D. Expression of the peripheral-type benzodiazepine receptor and apoptosis induction in hepatic stellate cells. *Gastroenterology* 2001;120:1212–26.
- [23] Fennell DA, Corbo M, Pallaska A, Cotter FE. Bcl-2 resistant mitochondrial toxicity mediated by the isoquinoline carboxamide PK11195 involves de novo generation of reactive oxygen species. *Br J Cancer* 2001;84:1397–404.
- [24] Berson A, Descatoire V, Sutton A, Fau D, Maulny B, Vadrot N, et al. Toxicity of alpidem, a peripheral benzodiazepine receptor ligand, but not zolpidem, in rat hepatocytes: role of mitochondrial permeability transition and metabolic activation. *J Pharmacol Exp Ther* 2001;299:793–800.
- [25] Halestrap AP, McStay GP, Clarke SJ. The permeability transition pore complex: another view. *Biochimie* 2002;84:153–66.
- [26] Crompton M, Barksby E, Johnson N, Capano M. Mitochondrial intermembrane junctional complexes and their involvement in cell death. *Biochimie* 2002;84:143–52.
- [27] Crompton M. Mitochondrial intermembrane junctional complexes and their role in cell death. *J Physiol* 2000;529(Pt 1):11–21.
- [28] van Loo G, Saelens X, van Gurp M, MacFarlane M, Martin SJ, Vandenabeele P. The role of mitochondrial factors in apoptosis: a Russian roulette with more than one bullet. *Cell Death Differ* 2002;9:1042.
- [29] Zamzami N, Kroemer G. The mitochondrion in apoptosis: how Pandora's box opens. *Nat Rev Mol Cell Biol* 2001;2:67–71.
- [30] Martinou JC, Green DR. Breaking the mitochondrial barrier. *Nat Rev Mol Cell Biol* 2001;2:63–7.
- [31] Kroemer G, Dallaporta B, Resche-Rigon M. The mitochondrial death/life regulator in apoptosis and necrosis. *Annu Rev Physiol* 1998;60:619–42.
- [32] Gottlieb RA. Mitochondria: execution central. *FEBS Lett* 2000;482:6–12.
- [33] Ricci JE, Gottlieb RA, Green DR. Caspase-mediated loss of mitochondrial function and generation of reactive oxygen species during apoptosis. *J Cell Biol* 2003;160:65–75.
- [34] Bono F, Lamarche I, Prabonnaud V, Le Fur G, Herbert JM. Peripheral benzodiazepine receptor agonists exhibit potent antiapoptotic activities. *Biochem Biophys Res Commun* 1999;265:457–61.
- [35] Strohmeier R, Roller M, Sanger N, Knecht R, Kuhl H. Modulation of tamoxifen-induced apoptosis by peripheral benzodiazepine receptor ligands in breast cancer cells. *Biochem Pharmacol* 2002;64:99–107.
- [36] Malgrange B, Rigo JM, Coucke P, Belachew S, Rogister B, Moonen G. Beta-carbolines induce apoptotic death of cerebellar granule neurones in culture. *Neuroreport* 1996;7:3041–5.
- [37] Bradford MM. A rapid and sensitive method for the quantitation of microgram quantities of protein utilizing the principle of protein-dye binding. *Anal Biochem* 1976;72:248–54.
- [38] Carre M, Andre N, Carles G, Borghi H, Brichese L, Briand C, et al. Tubulin is an inherent component of mitochondrial membranes that interacts with the voltage-dependent anion channel. *J Biol Chem* 2002;277:33664–9.
- [39] Stoeber PE, Carayon P, Casellas P, Portier M, Lavabre-Bertrand T, Cuq P, et al. Transient protection by peripheral benzodiazepine receptors during the early events of ultraviolet light-induced apoptosis. *Cell Death Differ* 2001;8:747–53.
- [40] Soldani C, Scovassi AI. Poly(ADP-ribose) polymerase-1 cleavage during apoptosis: an update. *Apoptosis* 2002;7:321–8.
- [41] Teitz T, Lahti JM, Kidd VJ. Aggressive childhood neuroblastomas do not express caspase-8: an important component of programmed cell death. *J Mol Med* 2001;79:428–36.
- [42] Kaufmann SH, Hengartner MO. Programmed cell death: alive and well in the new millennium. *Trends Cell Biol* 2001;11:526–34.
- [43] Beinlich A, Strohmeier R, Kaufmann M, Kuhl H. Relation of cell proliferation to expression of peripheral benzodiazepine receptors in human breast cancer cell lines. *Biochem Pharmacol* 2000;60:397–402.
- [44] Kletsas D, Li W, Han Z, Papadopoulos V. Peripheral-type benzodiazepine receptor (PBR) and PBR drug ligands in fibroblast and fibrosarcoma cell proliferation: role of ERK, c-Jun and ligand-activated PBR-independent pathways. *Biochem Pharmacol* 2004;67:1932.
- [45] Sgonc R, Gruber J. Apoptosis detection: an overview. *Exp Gerontol* 1998;33:525–33.
- [46] Grutter MG. Caspases: key players in programmed cell death. *Curr Opin Struct Biol* 2000;10:649–55.

- [47] Tsujimoto Y, Shimizu S. Bcl-2 family: life-or-death switch. *FEBS Lett* 2000;466:6–10.
- [48] He L, Lemasters JJ. Regulated and unregulated mitochondrial permeability transition pores: a new paradigm of pore structure and function? *FEBS Lett* 2002;512:1–7.
- [49] Vrabec JP, Lieven CJ, Levin LA. Cell-type-specific opening of the retinal ganglion cell mitochondrial permeability transition pore. *Invest Ophthalmol Vis Sci* 2003;44:2774–82.
- [50] Everett H, Barry M, Sun X, Lee SF, Frantz C, Berthiaume LG, et al. The myxoma poxvirus protein, M11L, prevents apoptosis by direct interaction with the mitochondrial permeability transition pore. *J Exp Med* 2002;196:1127–39.
- [51] Castedo M, Perfettini JL, Kroemer G. Mitochondrial apoptosis and the peripheral benzodiazepine receptor: a novel target for viral and pharmacological manipulation. *J Exp Med* 2002;196:1121–5.
- [52] Jayakumar AR, Panickar KS, Norenberg MD. Effects on free radical generation by ligands of the peripheral benzodiazepine receptor in cultured neural cells. *J Neurochem* 2002;83:1226–34.
- [53] Crompton M. The mitochondrial permeability transition pore and its role in cell death. *Biochem J* 1999;341(Pt 2):233–49.
- [54] Rebbaa A, Chou PM, Emran M, Mirkin BL. Doxorubicin-induced apoptosis in caspase-8-deficient neuroblastoma cells is mediated through direct action on mitochondria. *Cancer Chemother Pharmacol* 2001;48:423–8.
- [55] Fiers W, Beyaert R, Declercq W, Vandenabeele P. More than one way to die: apoptosis, necrosis and reactive oxygen damage. *Oncogene* 1999;18:7719–30.
- [56] Vercammen D, Brouckaert G, Denecker G, Van de CM, Declercq W, Fiers W, et al. Dual signaling of the Fas receptor: initiation of both apoptotic and necrotic cell death pathways. *J Exp Med* 1998;188:919–30.
- [57] Kawahara A, Ohsawa Y, Matsumura H, Uchiyama Y, Nagata S. Caspase-independent cell killing by Fas-associated protein with death domain. *J Cell Biol* 1998;143:1353–60.